Molecular Therapy
Nucleic Acids
Original Article

AMERICAN SOCIETY of GENE & CELL THERAPY

LRRK2 Antisense Oligonucleotides Ameliorate α-Synuclein Inclusion Formation in a Parkinson's Disease Mouse Model

Hien Tran Zhao,[1] Neena John,[2] Vedad Delic,[2] Karli Ikeda-Lee,[1] Aneeza Kim,[1] Andreas Weihofen,[3] Eric E. Swayze,[1] Holly B. Kordasiewicz,[1] Andrew B. West,[2] and Laura A. Volpicelli-Daley[2]

[1]Ionis Pharmaceuticals, Inc., Carlsbad, CA 92010, USA; [2]Center for Neurodegeneration and Experimental Therapeutics, University of Alabama, Birmingham, AL 35294, USA; [3]Biogen, Cambridge, MA 02142, USA

No treatments exist to slow or halt Parkinson's disease (PD) progression; however, inhibition of leucine-rich repeat kinase 2 (LRRK2) activity represents one of the most promising therapeutic strategies. Genetic ablation and pharmacological LRRK2 inhibition have demonstrated promise in blocking α-synuclein (α-syn) pathology. However, LRRK2 kinase inhibitors may reduce LRRK2 activity in several tissues and induce systemic phenotypes in the kidney and lung that are undesirable. Here, we test whether antisense oligonucleotides (ASOs) provide an alternative therapeutic strategy, as they can be restricted to the CNS and provide a stable, long-lasting reduction of protein throughout the brain. Administration of LRRK2 ASOs to the brain reduces LRRK2 protein levels and fibril-induced α-syn inclusions. Mice exposed to α-syn fibrils treated with LRRK2 ASOs show more tyrosine hydroxylase (TH)-positive neurons compared to control mice. Furthermore, intracerebral injection of LRRK2 ASOs avoids unwanted phenotypes associated with loss of LRRK2 expression in the periphery. This study further demonstrates that a reduction of endogenous levels of normal LRRK2 reduces the formation of α-syn inclusions. Importantly, this study points toward LRRK2 ASOs as a potential therapeutic strategy for preventing PD-associated pathology and phenotypes without causing potential adverse side effects in peripheral tissues associated with LRRK2 inhibition.

INTRODUCTION

Parkinson's disease (PD) is the second most common neurodegenerative disease. Pathological hallmarks of PD include accumulations of α-synuclein (α-syn) into Lewy bodies (LBs) and Lewy neurites (LNs), and progressive loss of dopaminergic (DA) neurons in the substantia nigra pars compacta (SNpc). Although the etiology of PD remains elusive, it is generally accepted that the formation and deposition of α-syn aggregates is a key step in PD pathogenesis.[1] Thus, factors influencing α-syn aggregation and degradation could be potential therapeutic targets.

Dominantly inherited mutations in *leucine-rich repeat kinase 2* (*LRRK2*) are the most common genetic cause of PD that is clinically indistinguishable from idiopathic PD.[2–4] LRRK2 protein contains multiple conserved domains and functions as both a guanosine triphosphatase (GTPase) and kinase.[5,6] All known pathogenic mutations in LRRK2 increase its kinase activity.[6–9] The structure of the LRRK2 kinase domain is similar to the mitogen-activated protein kinase kinase kinase (MAPKKK) domain, making it an attractive therapeutic target. As such, several LRRK2 kinase inhibitors are in preclinical development because of their promise in treating PD. Indeed, chronic administration of an LRRK2 kinase inhibitor in rats has been shown to protect against dopamine neuron loss in the SNpc induced by viral-mediated α-syn overexpression.[10] Currently, LRRK2 kinase inhibitor development focuses on generation of highly selective inhibitors that can cross the blood-brain barrier and are slowly metabolized. One reason the development of these inhibitors has proceeded with caution is that an examination of the lung tissue of monkeys treated with the LRRK2 kinase inhibitor GNE-7915 showed an expansion of lysosome-related organelles in type II pneumocytes.[11] While additional studies are required since GNE-7915 and the related GNE-0877 molecules also inhibit critical enzymes important for normal cellular function like TTK (dual-specificity tyrosine kinase), rodents with loss of LRRK2 expression show a similar lung phenotype.[11,12] It remains possible that a small molecule inhibitor of LRRK2 in the periphery may recapitulate the increased vacuolation of type 2 pneumocyte phenotypes associated with LRRK2 knockout (KO) mice and rats, potentially limiting this approach for neuroprotective strategies in PD.

Antisense oligonucleotides (ASOs) may provide an alternate strategy for blocking LRRK2 activity in the CNS while bypassing peripheral (i.e., systemic) effects. ASOs have recently emerged as promising strategies to treat multiple neurodegenerative diseases that can be readily

Received 25 April 2017; accepted 7 August 2017;
http://dx.doi.org/10.1016/j.omtn.2017.08.002.

Correspondence: Hien Tran Zhao, Neuroscience Drug Discovery, Ionis Pharmaceuticals, Inc., 2855 Gazelle Ct., Carlsbad, CA 92010, USA.
E-mail: hzhao@ionisph.com
Correspondence: Laura A. Volpicelli-Daley, Center for Neurodegeneration and Experimental Therapeutics, University of Alabama, Birmingham, AL 35294, USA.
E-mail: lvolpicellidaley@uabmc.edu

translated into the clinics. Indeed, nusinersen (SPINRAZA; Biogen), a centrally delivered ASO drug, was approved by the Food and Drug Administration (FDA) for treatment of spinal muscular atrophy, together with several other centrally delivered ASO therapeutics that are in clinical phase I trials for familial amyotrophic lateral sclerosis and Huntington's disease (ClinicalTrials.gov: NCT02193074, NCT02623699, and NCT02519036, respectively).[13–24] ASOs are single-stranded synthetic nucleic acids that bind target mRNA via Watson-Crick base pairing, resulting in degradation of target mRNA by RNase H, a ubiquitously expressed mammalian enzyme.[25] Phosphorothioate-modified deoxynucleotide (DNA) and 2′-O-methoxyethyl (2′-MOE) sugar modifications enable ASOs to be water soluble, resistant to exonucleases, and diffusible and to exhibit dose-dependent activity in vitro and in vivo.[26] Importantly, ASOs can be targeted directly to the brain by intracerebral ventricular injections and thus bypass adverse effects in the systemic organs. ASOs delivered to the brain show widespread distribution and cellular uptake and exhibit a long duration of action.[27–29]

In this study, we tested whether the ASO-mediated reduction of total levels of LRRK2 in the brain prevents phenotypes associated with PD. We demonstrate ASO-mediated LRRK2 suppression in both in vitro and in vivo model systems. Reducing levels of endogenous LRRK2 inhibits the recruitment of endogenously expressed α-syn into pathologic inclusions, recapitulating recent observations made with small molecule LRRK2 kinase inhibitors.[30] In addition, LRRK2 ASOs reduced the extent of DA cell loss and ameliorated α-syn-mediated motor defects. In contrast to the GNE series of LRRK2 kinase inhibitors, at therapeutically relevant doses, central delivery of LRRK2 ASOs does not affect LRRK2 levels in systemic organs such as the kidney and lung, which are sites where reduced LRRK2 activity might cause adverse phenotypes. Centrally delivered LRRK2 ASOs may provide a novel strategy to reduce LRRK2 activity in PD.

RESULTS

ASO-Mediated LRRK2 Suppression Prevented Pathologic α-Syn Formation in α-Syn Fibril-Treated Primary Neurons

We designed and screened ASOs complementary to *LRRK2* mRNA (n = 160) in SH-SY5Y cells (5 μM, 24 h) and *LRRK2* mRNA was assessed via qRT-PCR. While the non-targeting control sequence (CTL) had no effect on *LRRK2* mRNA (108.6% ± 2.6% compared to the untreated control [UTC]), two LRRK2-targeted sequences (SEQ1, SEQ2) resulted in 23.7% ± 7.2% and 26.5% ± 2.9% *LRRK2* mRNA compared to UTC, respectively (Figure 1A). These sequences were homologous for the human and mouse *Lrrk2* gene and were further optimized for use in primary neurons and in vivo and were thus subsequently termed ASO1 and ASO2.

We have previously shown that mutant G2019S-LRRK2 enhances formation of pathologic α-syn inclusions.[30] Treatment of both non-transgenic (Tg) neurons, with normal, endogenously expressed LRRK2 and G2019S-LRRK2-expressing neurons with LRRK2 inhibitors reduced α-syn aggregation, suggesting that both endogenous and mutant LRRK2 can contribute to α-syn accumulation. To further evaluate the impact of endogenous LRRK2 on α-syn aggregation, we employed ASOs to knock down LRRK2 expression. Primary neurons from non-Tg mice were treated at 7 days in vitro (DIV) with PBS, a control ASO (CTL), LRRK2 ASO1, or LRRK2 ASO2 at 3.0, 1.0, 0.3, and 0.1 μM, respectively. Eighteen days following treatment, immunoblots were performed for total LRRK2 levels. There was a substantial, stable reduction in LRRK2 protein produced by both ASO1 and ASO2 (Figure 1B). Next, we treated neurons with PBS, CTL, or LRRK2 ASO1 or ASO2 at 1 μM, together with 2 μg mL^{-1} α-syn pre-formed fibrils (PFFs) to induce inclusion formation. At 18 days post-treatment, neurons were fixed, and double immunofluorescence (IF) of phospho-S129 (pS129) α-syn antibody, a marker for α-syn inclusions,[31,32] and tau, an axonal marker, was performed (Figures 1C and 1D). Treatment with LRRK2 ASO1 or ASO2 significantly reduced the abundance of pS129-α-syn inclusions.

Central Delivery of ASOs Suppresses LRRK2 mRNA and Protein in the Brain without Affecting Kidney and Lung LRRK2 Levels

Because LRRK2 ASOs reduced pathologic α-syn in primary neuron cultures, we then tested whether they can reduce pathology in the brain, in vivo. Bolus intracerebral ventricular (ICVB) injection of ASOs into the lateral ventricles is an efficient method of ASO delivery.[29] To determine the potency of LRRK2 ASOs in vivo, wild-type C57BL/6J mice were treated with ASOs via ICVB, and tissues were harvested 14 days later. Both LRRK2 ASOs resulted in a dose-dependent reduction of *Lrrk2* mRNA in the dissected midbrain, an important PD brain region (Figures 2A and 2B). The ED_{50} for *Lrrk2* mRNA suppression was 351 μg for ASO1 and 283 μg for ASO2 in the midbrain. Expression of *Lrrk1* mRNA, a closely related family member, was not altered (Figure S1). Furthermore, we also measured the LRRK2 protein level via immunoblot in the midbrain of treated mice (Figures 2C and 2D). Both LRRK2 ASO1 and LRRK2 ASO2 produced a dose-dependent reduction of LRRK2 protein compared to PBS- and CTL-treated mice. A similar dose-dependent reduction of *Lrrk2* mRNA and LRRK2 protein was observed in the cortex (Figure S2). There were no changes in levels of total α-syn protein with any concentration of LRRK2 ASOs (Figures 2C and 2D).

To determine if the effects of ASOs in the CNS can be extended to longer time points, wild-type mice were treated with PBS, CTL ASO, or LRRK2 ASO1 and LRRK2 ASO2 at 700 μg via a single ICVB injection and were euthanized 56 days later (Figure 3A). While CTL ASO had no effect on *Lrrk2* mRNA in either the cortex (93.3% ± 2.6% compared to PBS) or midbrain (96.5% ± 15.2% compared to PBS), ASO1 and ASO2 resulted in significant mRNA suppression in both the cortex and midbrain of treated mice (Figure 3A). Taken together, central delivery of LRRK2 ASOs not only suppresses *Lrrk2* mRNA and LRRK2 protein in a dose-dependent manner but also results in long-lasting suppression in the CNS following a single injection.

To determine if central delivery of ASOs is specific to targeting LRRK2 in the CNS, we assessed *Lrrk2* mRNA in the kidney and lungs

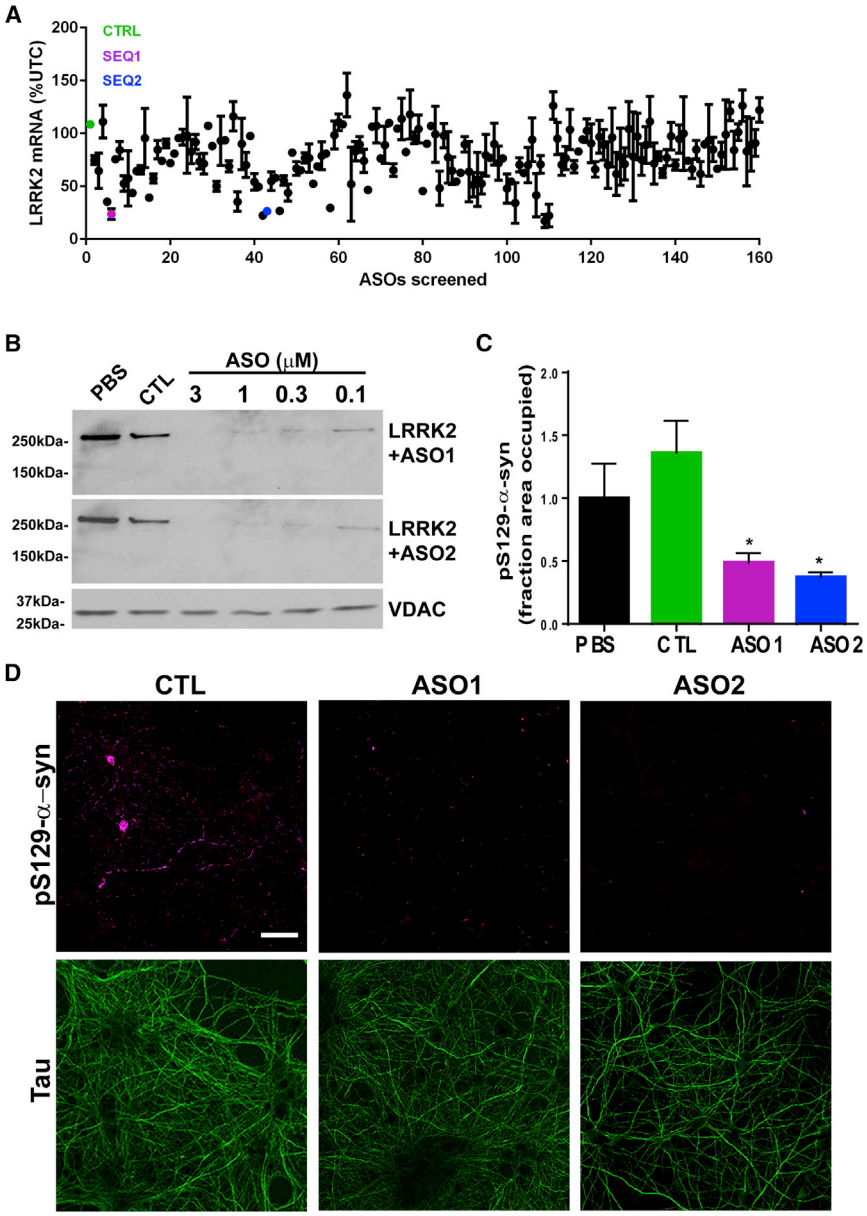

Figure 1. Identification of Efficacious LRRK2 ASOs that Reduce Formation of α-Syn Inclusions

(A) One-hundred and sixty different ASOs complementary to LRRK2 mRNA (5 μM) were added to SH-SY5Y cells. 24 hr later, *Lrrk2* mRNA was assessed via RT-qPCR (n = 2 per ASO). ASOs that reduced *Lrrk2* mRNA by more than 50% and that were homologous to both mouse and human LRRK2 are highlighted in blue and magenta. (B) Primary hippocampal neurons were treated at DIV7 with PBS, CTL ASO, or LRRK2 ASO1 or LRRK2 ASO2 at 3.0, 1.0, 0.3, and 0.1 μM. Eighteen days later, neurons were harvested and immunoblots were performed for total LRRK2 or voltage-dependent anion selective channel protein 1 (VDAC) as a loading control. (C) At DIV7, neurons were exposed to 2 μg mL^{-1} of sonicated PFFs with either PBS, CTL ASO, LRRK2 ASO1, or LRRK2 ASO1 at 1 μM. Eighteen days later, neurons were fixed, and IF was performed using an antibody to pS129-α-syn to visualize inclusions and tau to visualize axons. The fraction area occupied by pS129-α-syn was quantified using ImageJ. LRRK2 ASO-treated groups were compared to the PBS group using one-way ANOVA with Tukey's post-test. ***$p < 0.001$. Data represent mean ± SEM. (D) Representative intracerebral ventricular images of pS129-α-syn (magenta) and tau (green) in neurons treated with CTRL ASO, LRRK2 ASO1, or LRRK2 ASO2. The scale bar is 5 μm. VDAC, voltage-dependent anion channel protein.

of ICVB-treated mice. Since genetic ablation of LRRK2 resulted in the accumulation of autophagic vacuoles in proximal tubule epithelial cells in the kidney and type II pneumocytes in the lung,[33–35] we assessed the *Lrrk2* mRNA level in the kidney and lung of treated mice by qRT-PCR. Neither LRRK2 ASO affected *Lrrk2* mRNA in the kidney or lung when injected ICVB, although they produced a robust *Lrrk2* reduction in the brain (Figure 3A). Furthermore, H&E, Masson's trichrome stain, and LAMP2 immunohistochemistry (IHC) showed no abnormalities in the kidneys and lungs of treated mice (Figure S3). In summary, central delivery of ASOs specifically targets LRRK2 in the brain without affecting systemic LRRK2 levels.

Systemic Delivery of ASOs Reduces LRRK2 in the Kidney and Lungs without Affecting CNS LRRK2

We hypothesized that systemic delivery of ASOs only suppresses LRRK2 expression in systemic organs, since ASOs do not readily cross the blood-brain barrier. To test this hypothesis, we treated mice weekly for 8 weeks with 50 mg/kg per week of CTL, LRRK2 ASO1, or LRRK2 ASO2 via subcutaneous injections (Figure 3B). Tissues were harvested at 2 days after the last dose. While CTL ASO did not affect *Lrrk2* mRNA, ASO1 and ASO2 resulted in robust *Lrrk2* mRNA suppression in the kidney (Figure 3B). Both ASOs reduced lung *Lrrk2* mRNA, although the reduction was not statistically significant (Figure 3B). This is consistent with poor ASO delivery to the lung following introduction of ASOs into the systemic circulation.[27] Moreover, systemic delivery of ASOs did not affect midbrain *Lrrk2* mRNA levels (Figure 3B), in contrast to central delivery (Figure 3A).

Since genetic ablation of LRRK2 causes vacuolation in proximal epithelial cells in KO rodents,[12,33–35] we also examined the kidney of systemically ASO-treated mice histologically. In agreement with published data, we observed vacuoles in proximal epithelial cells of LRRK2 ASO-treated mice, but not PBS- or CTL-treated mice, by H&E and Masson's trichrome stain (Figure 4A). LAMP2 IHC also

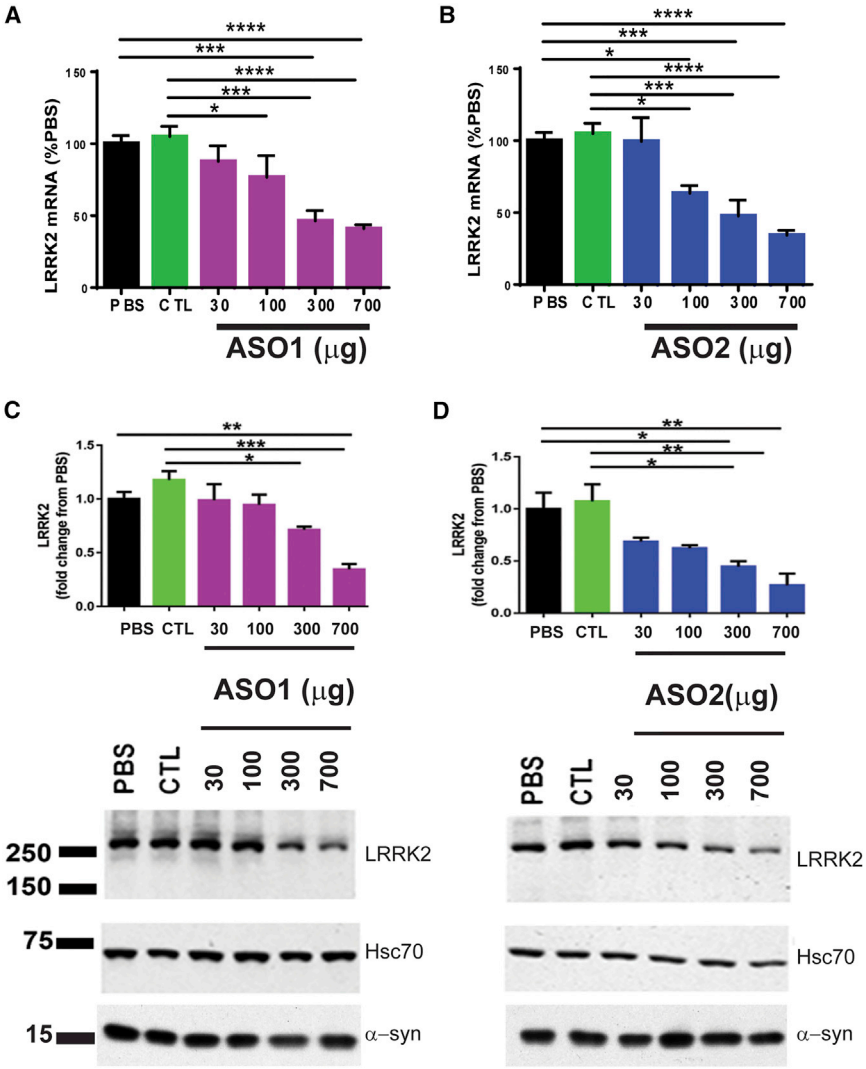

Figure 2. Central Administration of LRRK2 ASOs Reduces LRRK2 Levels in the Midbrain

(A and B) C57BL/6J mice received ICVB treatments with PBS (n = 3), 700 μg CTRL (n = 3), or LRRK2 ASO1 (n = 3) or LRRK2 ASO2 (n = 3) at 30, 100, 300, or 700 μg, respectively. Fourteen days later, brains were dissected. mRNA of midbrain LRRK2 was quantified by qRT-PCR for LRRK2 ASO1 (A) or LRRK2 ASO2 (B). (C and D) Midbrain homogenates from treated mice were immunoblotted for total LRRK2 or mouse α-syn. HSC70 was used as a loading control. Bands from the LRRK2 immunoblots were quantified using ImageJ and normalized to HSC70 for LRRK2 ASO1 (C) or LRRK2 ASO2 (D). Data represent the mean fold change relative PBS ± SEM. LRRK2 ASO-treated groups were compared to the PBS or CTL-ASO groups using one-way ANOVA with Tukey's post-test. *p < 0.05, **p < 0.01, ***p < 0.001. Data represent mean ± SEM.

showed an increase in late endosomes/lysosomes in proximal kidney epithelial cells. In the lung, LAMP2 IHC showed a mild increase in LAMP2-positive late endosomes/lysosomes, particularly with systemic treatment with ASO2 (Figure 4B). Taken together, systemic LRRK2 ASO administration resulted in LRRK2 suppression in the kidney and lung, with changes consistent with those found in the mouse LRRK2 KO.

ASO-Mediated LRRK2 Suppression Prevented Pathologic α-Syn Formation In Vivo

Previous work showed that intra-striatal injection of α-syn fibrils into non-Tg mice resulted in pS129-α-syn pathology in the substantia nigra.[36,37] LRRK2 kinase inhibitors reduce formation of α-syn inclusions in primary neurons.[30] We thus determined if ICVB injections of LRRK2 ASOs reduce α-syn inclusions in vivo. Mice first received injections of ASO1 or ASO2 with PBS as a control, followed by injection of PFFs (Figure 5A). Fifty-six days after injection with ASOs with or without PFFs, there remained a substantial reduction of *Lrrk2* mRNA in the contralateral midbrain (Figure 5B) and LRRK2 protein in the contralateral cortex (Figure 5C). No change in *Scna* mRNA, the gene encoding α-syn protein, was observed (Figure S4A). IHC for pS129-α-syn of the ipsilateral hemisphere to the injection site showed minimal staining in PBS-injected mice but revealed abundant inclusions in the SNpc of PFF-injected mice (Figure 5D). Furthermore, pS129-α-syn inclusions were found to colocalize with tyrosine hydroxylase (TH) in dopamine neurons (Figure 5E). Treatment with both LRRK2 ASO1 and LRRK2 ASO2 reduced the abundance of pS129-α-syn inclusions in the SNpc (Figure 5D). Quantitation of the number of somal inclusions revealed a significant (about 50%) reduction in pS129-α-syn inclusions in the SNpc of ASO1 and ASO2 treated mice (Figure 5F). We next performed sequential extraction of the contralateral cortex from control and PFF-injected mice in radioimmunoprecipitation assay buffer (RIPA) followed by 2% SDS to examine levels of total α-syn and pS129-α-syn. RIPA-soluble total α-syn levels were unaltered following LRRK2 ASO treatment, consistent with the finding that LRRK2 ASO did not affect the α-syn mRNA level (Figure S4A). No pS129-α-syn was observed in the RIPA-soluble fraction (Figure S4B), consistent with previous reports.[31,32] α-syn in LBs in diseased brains is insoluble in anionic detergents. It has been previously shown that PFFs cause a shift of normal α-syn into the insoluble SDS fraction,[31,32] and bilateral cortical pS129-α-syn pathology is evident following intra-striatal PFF inoculation.[31,38] We thus reasoned that pS129-α-syn in the SDS fraction from the contralateral cortex of the PFF-treated mice would provide further confirmation of the pS129-α-syn pathology observed in the SNpc. In control mice injected with PFFs, there was abundant pS129-α-syn in the insoluble

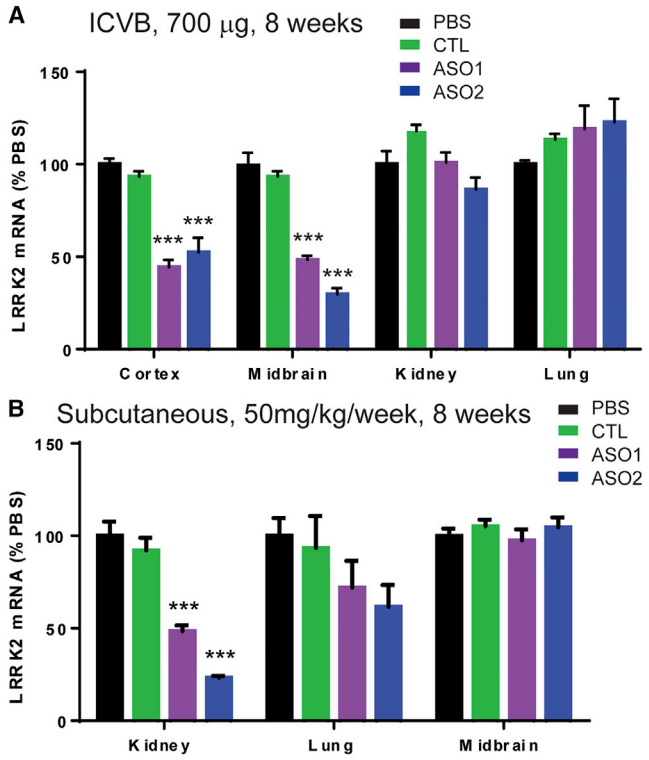

Figure 3. Effects of ICVB ASO Injections Compared to Systemic ASO Injections on LRRK2 Levels in the Brain, Kidney, and Lung

(A) C57BL/6J mice received ICVB treatments with PBS or 700 μg CTL ASO, LRRK2 ASO1, or LRRK2 ASO2. Fifty-six days later, the brain, lung, and kidney were dissected and mRNA of LRRK2 was quantified by qRT-PCR (n = 4). LRRK2 ASO-treated groups were compared to PBS or CTL-ASO groups using one-way ANOVA with Tukey's post-test. ***$p < 0.001$. (B) Mice received weekly subcutaneous injections of 50 mg/kg PBS, CTL ASO, LRRK2 ASO1, or LRRK2 ASO2 for 8 weeks. Two days after the last injection, tissues were harvested and mRNA was quantified in the kidney, lung, or midbrain by qRT-PCR (n = 4). LRRK2 ASO-treated groups were compared to the PBS- or CTRL-treated group using one-way ANOVA with Tukey's post-test. ***$p < 0.001$. Data represent mean ± SEM.

SDS fraction (Figure 5G). Both LRRK2 ASOs significantly reduced the accumulation of pS129-α-syn in the insoluble SDS fraction (Figure 5G), further confirming that the reduction of LRRK2 levels prevents the pathologic accumulation of α-syn. Consistent with published work,[36] α-syn PFFs resulted in a motor deficit, as demonstrated by reduced time remaining on the wire in injected mice compared to mice without PFF injection (Figure 5H). Importantly, ASO1 and ASO2 rescued this motor deficit.

Since the accumulation of α-syn aggregates in the SNpc compromises the survival of DA neurons over time,[31,36–39] we asked if long-term ASO-mediated LRRK2 suppression could be protective. To this end, another cohort of mice was treated with CTL ASO or LRRK2 ASO at 14 d before striatal PFF injection and again on day 90 following the first ASO ICVB, and they were euthanized at 180 d post-treatment (Figure 6A). In most of our in vivo studies, both ASO1 and ASO2 exhibit similar activity; however, ASO2 has a slightly better ED_{50} in the midbrain, as determined in Figure 2; thus, we chose this ASO for this study. Long-term ASO-mediated LRRK2 suppression was well tolerated, as mice gained weight normally and appeared healthy upon weekly physical examination until they were euthanized. Sustained *Lrrk2* mRNA and protein reduction was observed in ASO-treated mice at this time point (Figures 6B and 6C), while no change in *SNCA* mRNA was observed (Figure S4C). Furthermore, IHC analyses showed significant reduction in pS129-α-syn aggregates in the ipsilateral SNpc of LRRK2 ASO2-treated mice compared to CTL-treated mice (Figures 6D and 6E). To determine if LRRK2 suppression could reduce the loss of TH-expressing SNpc neurons at this time point, we conducted IHC using anti-TH antibody in CTL- and ASO2-treated mice. Quantification of TH-positive neurons showed that LRRK2 suppression resulted in a reduced loss of TH-positive cells in the ipsilateral SNpc of LRRK2 ASO2-treated mice compared to CTL-treated mice exposed to fibrils (Figures 6F and 6G). Taken together, ASO-mediated suppression of endogenous LRRK2 reduced motor behavior defects and pathological aggregation of α-syn and inhibited against TH cell loss in the PFF model.

DISCUSSION

In this study, we demonstrate the efficacy of LRRK2 ASOs in physiologically relevant in vitro and in vivo models of α-syn pathology. Particularly, we show that ASO-mediated suppression of endogenous LRRK2 not only reduces formation of pathologic α-syn inclusions in primary hippocampal neurons exposed to α-syn PFF, but it also ameliorates α-syn pathology in the SNpc and α-syn-associated motor deficit and DA toxicity following PFF inoculation in mice. Furthermore, we show that by only reducing LRRK2 levels in the brain, we can bypass potential adverse side effects of inhibiting LRRK2 function in the lung and kidney.

LRRK2 is one of the most promising therapeutic targets for the treatment of PD. The development of potent, selective LRRK2 kinase inhibitors that are brain penetrant has shown great progress in rat models of PD.[10] Our findings that either inhibiting LRRK2 activity[30] or reducing endogenous LRRK2 levels can abrogate α-syn pathology, reducing neuron death and motor defects, suggests that targeting LRRK2 may be an effective treatment not only for patients with LRRK2 mutations but also for individuals with idiopathic PD.

While genetic ablation of LRRK2 in rodents is generally well tolerated and exhibits no overt CNS phenotypes, KO animals exhibit enlarged kidneys and accumulation of vacuoles in proximal tubule epithelial cells[33–35] and in a subset of large epithelial cells, specifically type II pneumocytes.[33] Furthermore, oral delivery of LRRK2 inhibitors in non-human primates reduced LRRK2 activity in the brain but also caused vacuolation in type II pneumocytes in the lung.[11] Although it is unclear whether there are functional consequences to these changes, ultimately these systemic phenotypes may present liabilities for LRRK2 inhibition in clinical populations. Consistent with these reports, we showed that systemic administration of LRRK2 ASOs in mice resulted in significant LRRK2 suppression in the kidney and

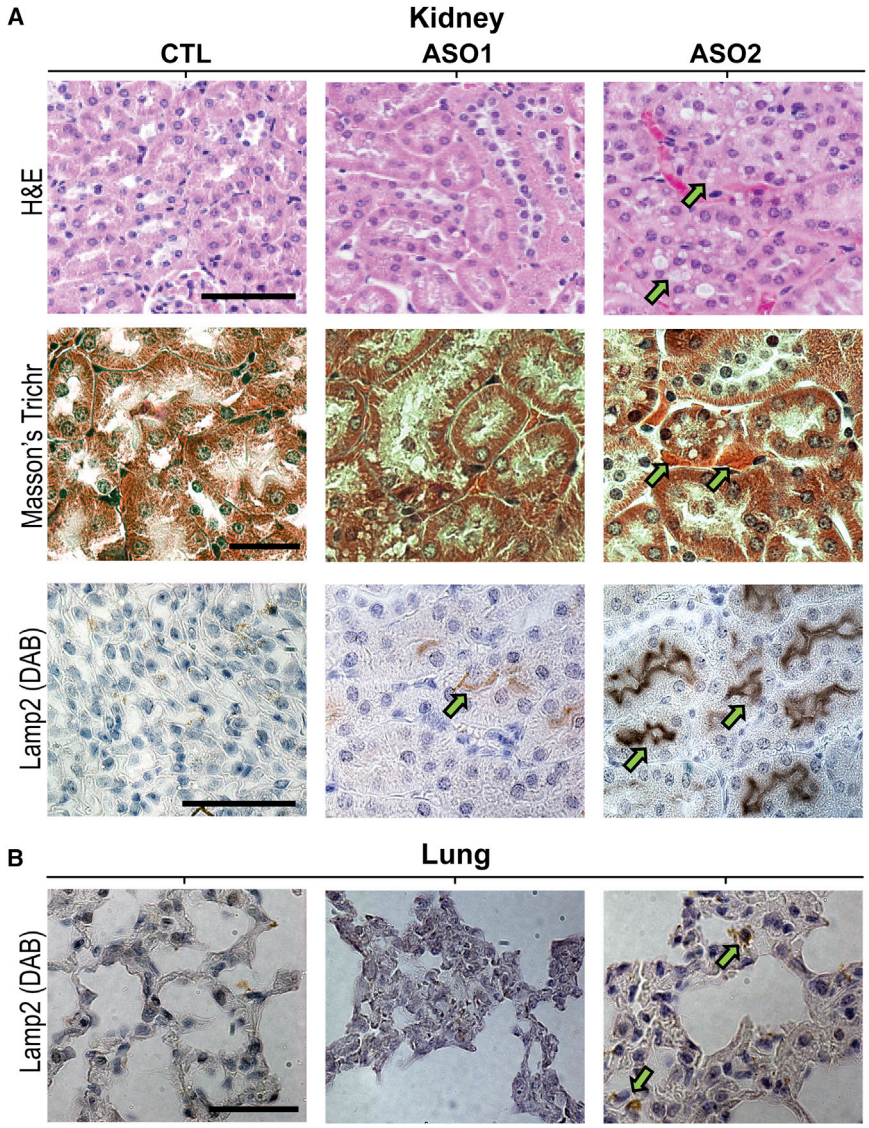

Figure 4. Systemic Administration of LRRK2 ASOs Recapitulates Some LRRK2 KO Phenotypes

(A) To visualize the presence of vacuoles in proximal kidney epithelial cells, sections from the kidney from mice systemically treated with CTL, LRRK2 ASO1, or LRRK2 ASO2 were stained using H&E (vacuoles indicated by green arrows) or Masson's trichrome stain to visualize protein deposits (orange coloration, indicated by green arrows). LAMP2 IHC was also performed to visualize late endosomes/lysosomes in tubule cells, with intense LAMP2 staining indicated with green arrows. (B) IHC for LAMP2 was also performed in lung tissue sections, with abnormal LAMP2 accumulations in pneumocytes indicated with green arrows. Sections shown are representative from dozens of sections cut through the kidney and lung from at least three animals from each group. Scale bars are 100 μm.

concomitant vacuolations in proximal tubule epithelial cells. No pathology was observed in the lung due to limited LRRK2 suppression. This was likely due to limited ASO exposure following subcutaneous injection in this organ compared to the kidney.[27] Moreover, central delivery of LRRK2 ASOs, while effectively reducing LRRK2 levels in the CNS, did not affect LRRK2 levels in the kidney or lung or cause vacuolation in these organs. Taken together, central delivery of LRRK2 ASOs is a superior route for ASO-mediated LRRK2 suppression compared to systemic administration, and this approach may be a viable therapeutic strategy for PD.

Our work furthers the understanding of mechanisms that may underlie the etiology of PD. Several new lines of evidence support the pathological interplay between LRRK2 and α-syn in the development of idiopathic PD (i.e., PD cases without LRRK2 mutations). First, in post-mortem studies, mutations in α-syn or LRRK2 result in typical cytoplasmic and neuritic α-syn accumulations in LBs and LNs, respectively.[40] Second, an increased LRRK2 protein level has been reported in PD brain regions with abundant LB pathology, in monocytes from PD cases, and in exosomes isolated from PD cases.[41–45] Third, in model systems, overexpression of either wild-type or PD-associated G2019S LRRK2 enhanced α-syn accumulation and downstream neuropathology in A53T α-syn mutant mice, and genetic ablation of LRRK2 not only reduced somatic α-syn accumulation but also significantly delayed A53T-induced neurodegeneration such as impaired microtubule dynamics and Golgi fragmentation.[46,47] Furthermore, genetic ablation of LRRK2 or treatment with a potent LRRK2 kinase inhibitor protected against DA cell loss caused by viral-mediated overexpression of α-syn.[10,48] Finally, in G2019S LRRK2-expressing primary neurons and rat DA neurons, α-syn aggregation was significantly increased following exposure to α-syn PFFs, and inhibition of LRRK2 kinase activity blocked this effect.[30] This study demonstrates that LRRK2-directed ASOs can capture some of the neuroprotection associated with the reduction of LRRK2 activity and/or expression following formation of α-syn inclusions in wild-type neurons and mice. Our approach administers LRRK2 ASOs prior to disease onset; since it takes up to 14 d for maximal LRRK2 mRNA and protein suppression with ASO, it remains to be determined if ASO administration is still effective in reducing α-syn pathology when the aggregation and neurodegeneration process has already been well established.

Our work also suggests an intrinsic function of LRRK2 in regulating α-syn pathology and its downstream effect and is in agreement with

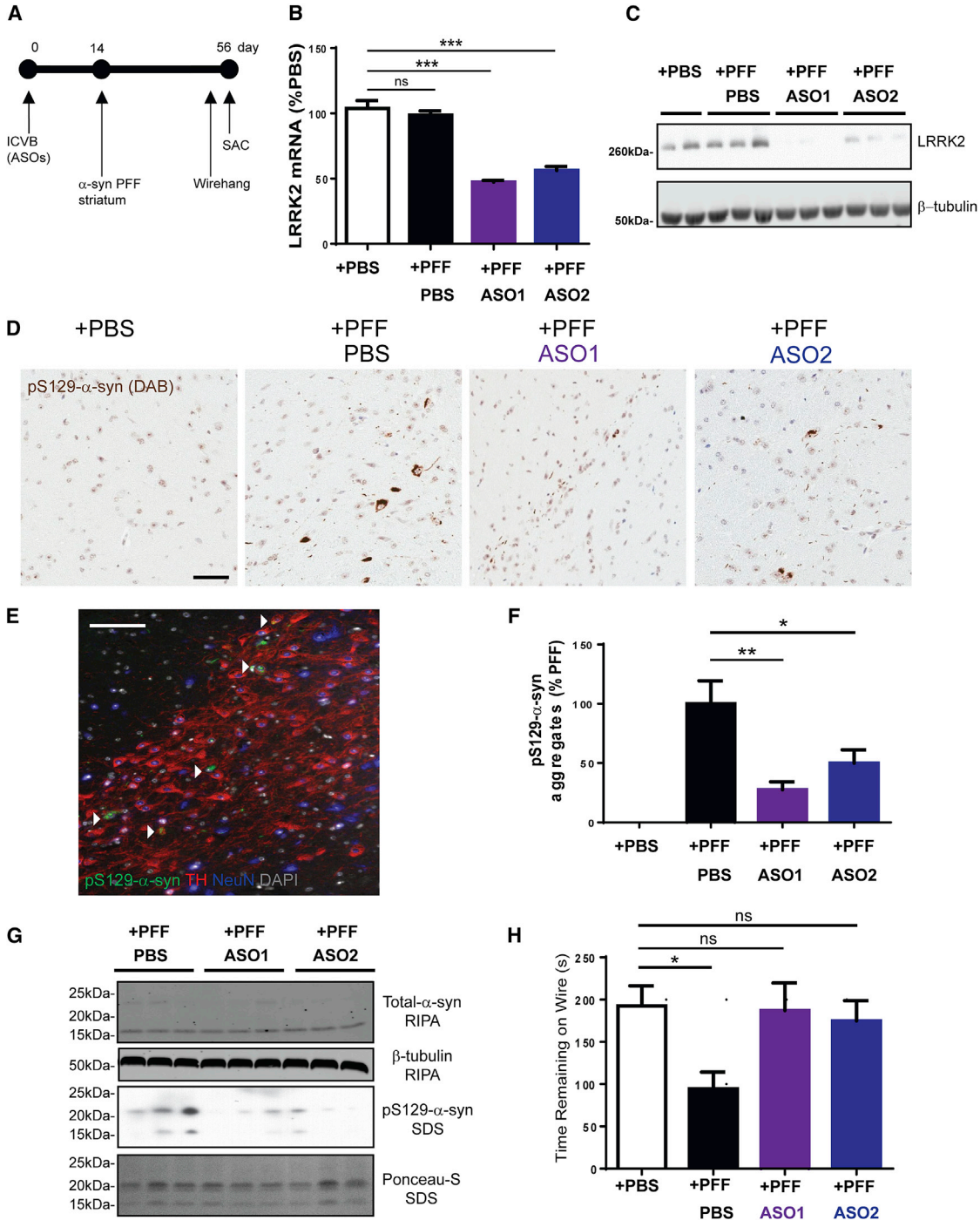

Figure 5. Centrally Administered LRRK2 ASOs Reduce Formation of α-Syn Inclusions

(A) Schematic of ASO injection, PFF injections, and the time point at which LRRK2 levels and α-syn pathology was assessed. Mice received ICVB injections of PBS, LRRK2 ASO1 (700 μg), or LRRK2 ASO2 (700 μg). Fourteen days later, 5 μg PFFs were unilaterally injected into the right striatum. Fifty-six days later, mice were euthanized. The injected hemisphere was fixed and embedded in paraffin for IHC. The midbrain from the contralateral side was harvested for mRNA quantitation and the contralateral cortex was harvested for protein analysis. (B) LRRK2 mRNA was analyzed by qRT-PCR (n = 11–12). LRRK2 ASO-treated groups were compared to the PFF/PBS control group using one-way ANOVA with Tukey's post-test. ***$p < 0.001$. Data represent mean ± SEM. (C) Total LRRK2 protein levels were analyzed by immunoblot. β-tubulin was used as a loading control. (D) IHC was performed on SNpc tissue sections using and antibody to pS129-α-syn to visualize inclusions. The scale bar is 50 μm. (E) Triple IF was performed to visualize pS129-α-syn inclusions in DA neurons positive for tyrosine hydroxylase (TH) and NeuN in PFF-injected mice. The scale bar is 50 μm. (F) The number of

(legend continued on next page)

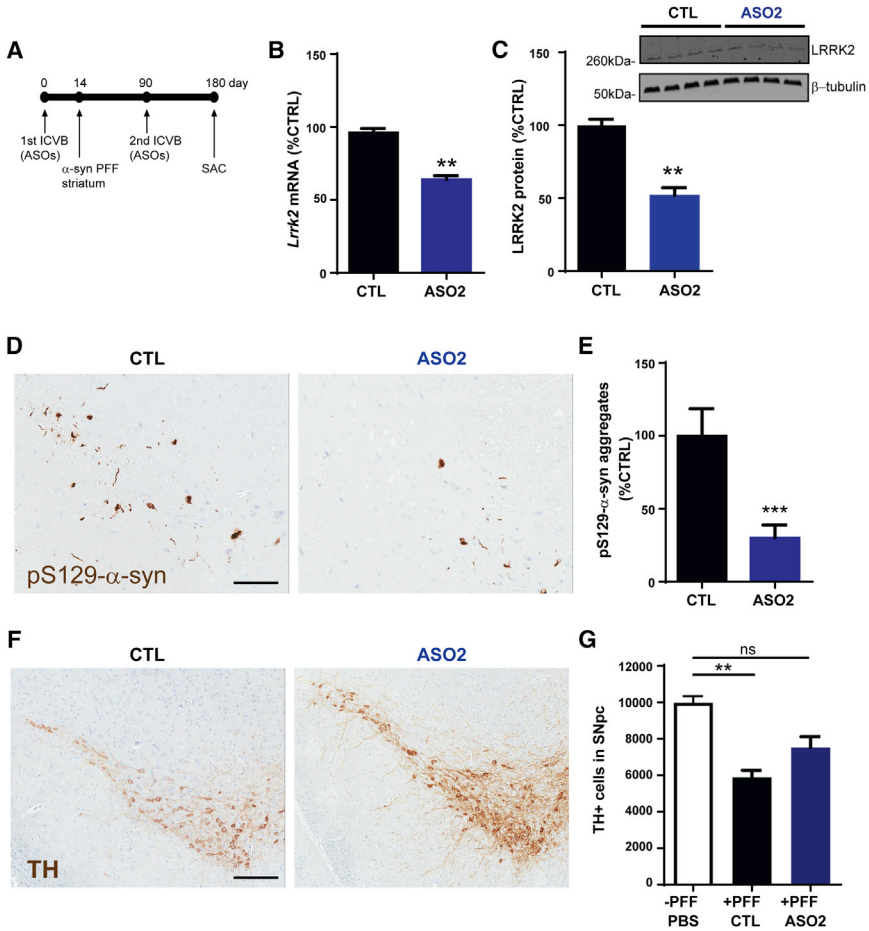

Figure 6. LRRK2 ASOs Preserve Dopamine Neurons in the SNpc after PFF Exposure Compared to Control ASOs

(A) Schematic of ASO injection, PFF injections, and time point which mice were euthanized for assessment of α-synuclein pathology and DA neurons. Mice received ICVB injections of CTL ASO (700 μg) or LRRK2 ASO2 (700 μg). Fourteen days later, 5 μg PFFs were unilaterally injected into the striatum. Ninety days later, mice received additional ICVB injections of CTL ASO (700 μg) or LRRK2 ASO2 (700 μg). The mice were euthanized 180 days after the first ASO injection. (B) The contralateral midbrain was harvested for mRNA quantitation. Levels of LRRK2 mRNA were quantified by qRT-PCR (n = 12). The LRRK2 ASO2 group was compared to CTL-ASO group using the unpaired t test. **$p < 0.01$. (C) The contralateral cortex was harvested for LRRK2 protein quantification by western blot; β-tubulin was used as a loading control (n = 4). The LRRK2 ASO2 group was compared to the CTL-ASO group using the unpaired t test. **$p < 0.01$. (D) IHC using an antibody to pS129-α-syn was performed in the midbrain from the injected side of the brain to visualize inclusions. (E) The number of somal of pS129-α-syn inclusions was quantified from SNpc from mice that received ICVB injections of CTL ASO or LRRK2 ASO2 followed by striatal injection of PFFs. The LRRK2 ASO2 group was compared to the CTL-ASO group using the unpaired t test. ***$p < 0.001$. (F) IHC using an antibody to tyrosine hydroxylase to visualize TH-positive neurons in PFF-treated mice receiving CTL- or LRRK2 ASO2. (G) Quantitation of TH-positive neurons in the SNpc of non-PFF-treated mice (n = 2) or in PFF-treated mice receiving CTL or LRRK2 ASO2 (n = 6). PFF-treated groups were compared to the PBS control group using one-way ANOVA with Dunnett's post-test. **$p < 0.01$. Scale bars are 50 μm. ns, not significant. Data represent mean ± SEM.

previous studies that demonstrated benefits of LRRK2 KO in various contexts of α-syn-mediated toxicity. Interestingly, a recent study showed that mutant LRRK2 toxicity in induced pluripotent neurons derived from patients with PD did not require LRRK2 kinase activity or inclusion bodies, but instead depended on LRRK2 levels and α-syn expression.[49] Together with this study, our findings provide further support for inhibition of LRRK2 expression as a therapeutic strategy to ameliorate LRRK2- and α-syn-induced neurodegeneration, in addition to α-syn pathology. Remarkably, an acute 40%–50% reduction in LRRK2 mRNA appears sufficient to reduce α-syn aggregation and α-syn-induced cell death in our PD model.

Although one study showed that LRRK2 and α-syn mRNA was co-regulated in the mouse striatum,[50] it is unlikely that LRRK2 influences α-syn aggregation at the mRNA level, since we did not observe any change in the *Snca* mRNA level following LRRK2 suppression in vivo. It is possible that LRRK2 exerts its effect once PFF-induced α-syn aggregates have formed, particularly in protein clearance pathways. Consistent with this hypothesis, LRRK2 has been implicated in degradative processes[51] and was reported to have an inhibitory effect on chaperone-mediated autophagy, a mechanism reported to degrade α-syn.[52] Likewise, removing endogenous LRRK2 could enhance the degradation of aggregated α-syn, thereby

somal pS129-α-syn inclusions was quantified from SNpc from PBS-injected mice and from mice that received ICVB injections of PBS with striatal injections of PFFs or mice that received ICVB injections of LRRK2 ASO1 or LRRK2 ASO2 followed by striatal injection of PFFs. LRRK2 ASO-treated groups were compared to the PFF/PBS control group using one-way ANOVA with Tukey's post-test. *$p < 0.05$, **$p < 0.01$. Data represent mean ± SEM. (G) Cortical tissue from mice that received ICVB injections of PBS, LRRK2 ASO1, or LRRK2 ASO2 followed by striatal injection of PFFs was sequentially extracted. First, lysates were prepared by homogenization in RIPA buffer. RIPA-soluble fractions were resolved by SDS-PAGE and immunoblots were performed using an antibody to total α-syn and β-tubulin was used as a loading control. The lysates were then spun at high speed and the resulting pellets were resuspended in 2% SDS. This insoluble fraction was resolved by SDS-PAGE and immunoblots were performed using an antibody to pS129-α-syn. Ponceau staining of the immunoblot demonstrates equal loading of the samples. (H) The wire hang behavioral test was performed 56 days after fibril injections. The latency of mice to fall off the wire grid was recorded and averaged over two trials (15 min apart). PFF-treated groups were compared to the PBS control group using one-way ANOVA with Tukey's post-test. *$p < 0.05$. ns, not significant.

Table 1. Sequences of Oligonucleotides Used

Oligonucleotide	Target	Sequence	Experiment
SEQ1	LRRK2	GGACTGCTCTCTTTCTCACA	in vitro SH-SY5Y
SEQ2	LRRK2	TCCACATTTCTGAATCCCAG	in vitro SH-SY5Y
CTL	NA	GTGCGCGCGAGCCCGAAATC	in vitro SH-SY5Y
ASO1	LRRK2	GGACTGCTCTCTTTCTCACA	primary neurons, in vivo
ASO2	LRRK2	TCCACATTTCTGAATCCCAG	primary neurons, in vivo
CTL	NA	CCTATAGGACTATCCAGGAA	primary neurons, in vivo

Underlined letters indicate 2′-O-methoxyethyl (MOE)-modified bases. Italicized letters indicate the phosphodiester backbone.

resulting in less cytoplasmic α-syn accumulation in our PD model. Another possibility is that LRRK2 may influence α-syn intracellular trafficking and somatic accumulation. In support of this view, Lin et al.[47] showed that removing endogenous LRRK2 in α-syn A53T transgenic mice significantly reduced Golgi fragmentation, accumulations of ubiquitinated proteins including α-syn. Further investigations into the molecular mechanism underlying the protective effect of LRRK2-targeting ASOs in model systems will be required. Our results further support a role for LRRK2 in the formation of α-syn pathology and neurodegeneration and demonstrate that ASO-mediated LRRK2 suppression can be a potential therapy for α-syn-mediated PD.

MATERIALS AND METHODS

Oligonucleotides

Synthesis and purification of all chemically purified ASOs was performed as previously described.[53] Sequence 1 and sequence 2 (SEQ1 and SEQ2) were uniform 20-mer gapmer phosphorothioate oligonucleotides containing 2′-MOE groups at positions 1–5 and 15–20. ASO1 and ASO2 had the same sequences and chemistry design as SEQ1 and SEQ2 except with a mixed phosphorothioate and phosphodiester backbone (denoted in Table 1). The sequences evaluated are listed in Table 1.

Animals

All experimental procedures involving animals were performed in accordance with Institutional Animal Care and Use Committee guidelines, were approved by the University of Alabama at Birmingham's Institutional Animal Care and Use Committee, and were in accordance with the National Institutes of Health Guide for the Care and Use of Laboratory Animals (publication no. 80-23). Adult wild-type C57BL/6J mice were obtained from The Jackson Laboratory (Bar Harbor, ME) for in vivo screening and characterizations of ASOs. Pregnant CD1 dams were purchased from Charles River (Wilmington, MA) for primary neuronal cultures. Adult wild-type C57BL6/C3H mice were purchased from Charles River (Wilmington, MA) for PFF inoculation studies.

Intracerebral Ventricular Injection and Subcutaneous Injection of ASOs and Striatal α-syn PFF Injection

Lyophilized ASOs were dissolved in sterile phosphate-buffered saline without calcium or magnesium and quantified by UV spectrometry. ASOs were then diluted to desired concentration and sterilized through at 0.2-μm filter. For central delivery studies, a single intracerebral ventricular bolus (ICVB) injection was performed as described with two modifications.[29] First, coordinates for the right lateral ventricle injection were as follows: anterior-posterior (AP), −0.3 mm; medial-lateral (ML), 1 mm; and dorsal-ventral (DV), −3.0 mm. Second, 10 μL ASO solution was injected once at a rate of 1 μL/s. For the dose-response ICVB study, wild-type C57BL/6J female mice (n = 3) aged 8–10 weeks were injected with PBS, CTL ASO at 700 μg, or ASO1 or ASO2 at 30, 100, 300, and 700 μg. Mice were euthanized at 14 days post-ICVB injection. For the 8-week study, wild-type C57BL/6J female mice (n = 4) received a single ICVB injection at 700 μg and were euthanized at 56 days post-dose. For systemic studies, wild-type C57BL/6J female mice (n = 4) received subcutaneous bolus injections of PBS, CTL ASO, ASO1, or ASO2 at 50 mg/kg weekly for 8 weeks and were euthanized at 2 days after the last dose. In the short-term proof-of-concept experiment, the ICVB injection of saline, ASO1 (700 μg), or ASO2 (700 μg) was performed 2 weeks before striatal α-syn PFF inoculation into the right ventricle and right striatum, respectively. Wild-type C57BL6/C3H mice (n = 12) were used. α-syn PFF was prepared from recombinant mouse α-syn as described.[36] The striatal injection of 5 μg α-syn PFF in 2 μL dosing solution was performed as previously described.[31,36] Mice were tested on the wire hang task on day 55 and euthanized on day 56 post-ICVB injection. For the long-term proof-of-concept experiment, mice received ASOs and PFF injections just as in the short-term experiment, except they received a second ICVB injection on day 90 and were euthanized on day 180 after the 1st ICVB.

RT-PCR

Cultured cells were lysed in 300 μL RLT buffer containing 1% (v/v) 2-mercaptoethanol (BME; Sigma-Aldrich). A 2-mm coronal section of the cortex at 1 mm posterior to the injection site or a 3-mm posterior brain coronal section containing the midbrain was dissected and homogenized in 500 μL guanidine isothiocyanate solution (Invitrogen) supplemented 8% BME. The entire kidney and 1 leaflet of the lung were homogenized in 1 mL of 1% BME/RLT buffer. Twenty microliters of lysates was used for RNA isolation using the RNeasy 96 kit per the manufacturer's instructions (QIAGEN). RT-PCR was done using a StepOne real-time PCR system (Applied Biosystems), as described previously.[54] The following sequences of primers and probes were used: mouse *Lrrk2*: 5′-GGCGAGTTA TCCGCACCAT-3′ (forward), 5′-CCAAAACCAGCATGACATTC TTAA-3′ (reverse), and 5′-Fam-GAGAGCCATGGCCACAGCA CAA-Tamra-3′ (probe); and mouse *Lrrk1*: 5′-CTGCTCAGGAAG TATTTCATCGAA-3′ (forward), 5′-GGGACCATTTCACACGAA GTG-3′ (reverse), and 5′-Fam-GGGACCATTTCACACGAAGTG-Tamra-3′ (probe). PCR results were normalized by housekeeping genes, *cyclophilin A* or *Gapdh*, and were further normalized to the level in PBS-treated mice or untreated cells.

In Vitro Cell Cultures in SH-SY5Y Cultures and Primary Neurons

SH-SY5Y cells were cultured in 1:1 mixture of Eagle's minimum essential medium and F12 medium, supplemented with 10% FBS in a 96-well plate at 10^4 cells/well. Oligonucleotides were transfected at 5 μM with cytofectamine per the manufacturer's instructions (Invitrogen, CA), and cells were harvested at 24 hr post-treatment for RNA extraction and mouse LRRK2 mRNA quantification by qRT-PCR.

Primary hippocampal cultures were prepared from E16–E18 C57BL/6J mouse brains and maintained as described.[32,55] Fibril transduction was performed at 7 DIV at 2 μg/mL, together with 0.3 or 1 μM ASOs, as described.[30] Each experiment was performed in duplicate and repeated 3–5 times. Transduced neurons were harvested at 18 days post-transduction for indirect IF with pS129 α-syn antibody (81A; gift from Virginia Lee) for α-syn pathology and with tau (Dako) for neuronal density. The fraction area occupied was quantified using ImageJ software (NIH) as previously described.[30]

Histology Analyses

Mice were euthanized at the end of each study by CO_2 affixation, followed by transcardial perfusion with ice-cold PBS. For 8-week ICVB and systemic studies, the left hemibrain, lung, and kidney were extracted, fixed overnight in 10% normal buffered saline (NBF), and embedded in paraffin. Serial sections 5 μm thick were cut from the formalin-fixed, paraffin-embedded tissue blocks and floated onto charged glass slides and dried overnight at 60°C. An H&E-stained section and a Masson's trichrome-stained slide were obtained from each tissue block. All sections for IHC were deparaffinized and hydrated using graded concentrations of ethanol to deionized water. The tissue sections were subjected to antigen retrieval by 0.01 M Tris/1 mM EDTA buffer (pH 9) with a pressure cooker for 5 min (preheat buffer for 10 min). Following antigen retrieval, all sections were washed gently in deionized water and then transferred into 0.05 M Tris-based solution in 0.15 M NaCl with 0.1% (v/v) Triton X-100, pH 7.6 (TBST). Endogenous peroxidase was blocked with 3% hydrogen peroxide for 20 min. To further reduce nonspecific background staining, slides were incubated with 3% normal goat serum for 30 min (Sigma) at room temperature. All slides were then incubated at 4°C overnight with rabbit anti-mouse LAMP-2 antibody (H-207) (1:25, SC5571; Santa Cruz). After washing with TBST, sections then incubated with goat anti-rabbit immunoglobulin G (IgG)-horseradish peroxidase (HRP) (1:300, SC2004; Santa Cruz). Diaminobenzidine (DAB; ScyTek Laboratories, Logan, UT) was used as the chromagen and hematoxylin (no. 7211; Richard-Allen Scientific) was used as the counterstain.

For the combined ICVB and PFF study, the right hemisphere (site of PFF inoculation) was extracted, fixed overnight in 70% ethanol in 150 mM NaCl, and embedded in paraffin. 6-μm coronal sections were collected through the entire CNS (brain, brain stem), as described.[31] Tissues were deparaffinized and rehydrated as above and were subjected to antigen retrieval by sodium citrate buffer at pH 6 (H-3300; Vector Laboratories) with a pressure cooker for 5 min (preheat buffer for 10 min). For assessment of pathologic α-syn aggregates, every 10th section was stained with pS129-α-syn antibody (Ab51253; Abcam), as described.[31] Numbers of pS129-α-syn-positive cells in the SNpc were quantified in a blinded manner by two independent raters. Both intra-rater and inter-rater reliability were ≥90% (data not shown). For assessment of DA SNpc neurons, every 10th section was stained by IHC with anti-TH antibody (P40101-0; Pel-Freez), as described.[31] TH-positive neurons in the SNpc were manually counted by an investigator who was blinded to the treatment condition.

Triple IF of TH, pS129-α-syn, and NeuN was done sequentially using an OPAL 7-color fIHC kit (PerkinElmer), per the manufacturer's instructions.

Western Blot

For the 2-week ICVB dose-response study and the 8-week ICVB study, a 2-mm coronal cortex section posterior to the site of cortex dissection for RNA was dissected. Tissues were sonicated in 1× RIPA buffer (25 mM Tris, pH 7.5, 150 mM NaCl, 0.1% SDS, and 1% Triton X-100) containing protease and phosphatase inhibitor cocktails (9806; Cell Signaling Technology) and were spun at 16,000 × *g* for 30 min at 4°C. For the ICVB and PFF study, pellets were subsequently washed and resuspended in 2% SDS in Tris-buffered saline (TBS). The protein concentration was determined by the Bradford or bicinchoninic acid assay (BCA) protein assay (Pierce). Samples were separated on 7.5% gels and were blotted with MJFF2 for LRRK2 (133474; Abcam) or separated on 4%–12% Bis-Tris gels and blotted with Syn1 for total mouse α-syn (610786; BD Transductions), pS129-α-syn for pathologic α-syn (Ab51253; Abcam). Primary antibodies were detected with corresponding secondary antibodies conjugated to horseradish peroxidase (Jackson ImmunoResearch), and blots were developed by enhanced chemiluminescence (GE Amersham).

Wire Hang Task

To assess grip strength, the wire hang task was performed as described, with slight modifications.[31] Briefly, mice were acclimatized to the testing environment 4 hr before the actual test. The test was performed by an investigator blinded to the treatment conditions. Mice were placed on a standard wire cage lid on top of clean cages with bedding, and they were allowed to walk around for 2 min. Wire tops were gently agitated and flipped upside down to cause the animals to grip the wires. The latency of mice to fall off the grid was recorded and averaged over two trials (15 min apart). Trials were stopped if mice remained on the lid for over 5 min.

Statistical Analyses

For pairwise comparisons, Student's t tests were used. For comparisons of more than 2 treatment groups, one-way ANOVA with Dunnett's or Tukey's post hoc tests was used. Statistical significance was set at $p < 0.05$. Data are presented as the mean ± SEM unless otherwise indicated.

SUPPLEMENTAL INFORMATION

Supplemental Information includes four figures and can be found with this article online at http://dx.doi.org/10.1016/j.omtn.2017.08.002.

AUTHOR CONTRIBUTIONS

H.T.Z., H.B.K., E.E.S., and L.A.V.-D. conceived and coordinated the study. H.T.Z., L.A.V.-D., N.J., V.D., K.I.-L., A.K., A.W., and A.B.W. designed, performed, and analyzed the experiments. H.T.Z., L.A.V.-D., and A.B.W. wrote the paper with input from all authors. All authors analyzed the results and approved the final version of the manuscript.

CONFLICTS OF INTEREST

H.T.Z., H.B.K, E.E.S., K.I.-L., and A.K. are paid employees and stockholders of Ionis Pharmaceuticals Inc. (Carlsbad, CA). A.W. is a paid employee and stockholder of Biogen (Cambridge, MA). N.J., V.D., A.B.W., and L.A.V.-D. have no conflicts of interest.

ACKNOWLEDGMENTS

We thank Dr. Virginia Lee for the 81A antibody, Dr. Warren Hirst for a critical review of the manuscript, Dr. Tracy Cole for thoughtful discussions, and Yuhong Jiang, Jose Mendosa, Gemma Ebeling, and Johnnatan Tamayo for technical assistance. This work was supported in part by the NIH (grants R01-NS064934-06 and R21-NS097643-01 to A.B.W.).

REFERENCES

1. Trojanowski, J.Q., and Lee, V.M. (1998). Aggregation of neurofilament and alpha-synuclein proteins in Lewy bodies: implications for the pathogenesis of Parkinson disease and Lewy body dementia. Arch. Neurol. *55*, 151–152.
2. Paisàn-Ruìz, C., Sàenz, A., Lòpez de Munain, A., Martì, I., Martìnez Gil, A., Martì-Massò, J.F., and Pèrez-Tur, J. (2005). Familial Parkinson's disease: clinical and genetic analysis of four Basque families. Ann. Neurol. *57*, 365–372.
3. Zabetian, C.P., Samii, A., Mosley, A.D., Roberts, J.W., Leis, B.C., Yearout, D., Raskind, W.H., and Griffith, A. (2005). A clinic-based study of the LRRK2 gene in Parkinson disease yields new mutations. Neurology *65*, 741–744.
4. Zimprich, A., Biskup, S., Leitner, P., Lichtner, P., Farrer, M., Lincoln, S., Kachergus, J., Hulihan, M., Uitti, R.J., Calne, D.B., et al. (2004). Mutations in LRRK2 cause autosomal-dominant parkinsonism with pleomorphic pathology. Neuron *44*, 601–607.
5. Liu, G., Aliaga, L., and Cai, H. (2012). α-synuclein, LRRK2 and their interplay in Parkinson's disease. Future Neurol. *7*, 145–153.
6. West, A.B., Moore, D.J., Biskup, S., Bugayenko, A., Smith, W.W., Ross, C.A., Dawson, V.L., and Dawson, T.M. (2005). Parkinson's disease-associated mutations in leucine-rich repeat kinase 2 augment kinase activity. Proc. Natl. Acad. Sci. USA *102*, 16842–16847.
7. Steger, M., Tonelli, F., Ito, G., Davies, P., Trost, M., Vetter, M., Wachter, S., Lorentzen, E., Duddy, G., Wilson, S., et al. (2016). Phosphoproteomics reveals that Parkinson's disease kinase LRRK2 regulates a subset of Rab GTPases. eLife *5*, e12813.
8. West, A.B., and Cookson, M.R. (2016). Identification of bona-fide LRRK2 kinase substrates. Mov. Disord. *31*, 1140–1141.
9. West, A.B., Moore, D.J., Choi, C., Andrabi, S.A., Li, X., Dikeman, D., Biskup, S., Zhang, Z., Lim, K.L., Dawson, V.L., and Dawson, T.M. (2007). Parkinson's disease-associated mutations in LRRK2 link enhanced GTP-binding and kinase activities to neuronal toxicity. Hum. Mol. Genet. *16*, 223–232.
10. Daher, J.P., Abdelmotilib, H.A., Hu, X., Volpicelli-Daley, L.A., Moehle, M.S., Fraser, K.B., Needle, E., Chen, Y., Steyn, S.J., Galatsis, P., et al. (2015). Leucine-rich repeat kinase 2 (LRRK2) pharmacological inhibition abates α-synuclein gene-induced neurodegeneration. J. Biol. Chem. *290*, 19433–19444.
11. Fuji, R.N., Flagella, M., Baca, M., Baptista, M.A., Brodbeck, J., Chan, B.K., Fiske, B.K., Honigberg, L., Jubb, A.M., Katavolos, P., et al. (2015). Effect of selective LRRK2 kinase inhibition on nonhuman primate lung. Sci. Transl. Med. *7*, 273ra15.
12. Baptista, M.A., Dave, K.D., Frasier, M.A., Sherer, T.B., Greeley, M., Beck, M.J., Varsho, J.S., Parker, G.A., Moore, C., Churchill, M.J., et al. (2013). Loss of leucine-rich repeat kinase 2 (LRRK2) in rats leads to progressive abnormal phenotypes in peripheral organs. PLoS ONE *8*, e80705.
13. Single and Multiple Dose Study of BIIB067 in Adults with Amyotrophic Lateral Sclerosis (ALS). https://ClinicalTrials.gov/show/NCT02623699.
14. Safety, Tolerability, Pharmacokinetics, and Pharmacodynamics of IONIS-HTTRx in Patients with Early Manifest Huntington's Disease. https://ClinicalTrials.gov/show/NCT02519036.
15. An Open-Label Safety, Tolerability, and Dose-Range Finding Study of Nusinersen (ISIS 396443) in Participants with Spinal Muscular Atrophy (SMA) (SMNRx). https://ClinicalTrials.gov/show/NCT01494701.
16. An Open-Label Safety, Tolerability and Dose-Range Finding Study of Multiple Doses of Nusinersen (ISIS 396443) in Participants with Spinal Muscular Atrophy. https://ClinicalTrials.gov/show/NCT01703988.
17. An Open-Label Safety and Tolerability Study of Nusinersen (ISIS 396443) in Participants with Spinal Muscular Atrophy Who Previously Participated in ISIS 396443-CS1 (NCT01494701). https://ClinicalTrials.gov/show/NCT01780246.
18. An Open-Label Safety and Tolerability Study of Nusinersen (ISIS 396443) in Participants with Spinal Muscular Atrophy (SMA) Who Previously Participated in ISIS 396443-CS2 (NCT01703988) or ISIS 396443-CS10 (NCT01780246). https://ClinicalTrials.gov/show/NCT02052791.
19. A Study to Assess the Efficacy, Safety and Pharmacokinetics of Nusinersen (ISIS 396443) in Infants with Spinal Muscular Atrophy (SMA). https://ClinicalTrials.gov/show/NCT01839656.
20. A Study for Participants with Spinal Muscular Atrophy (SMA) Who Previously Participated in Nusinersen (ISIS 396443) Investigational Studies (SHINE). https://ClinicalTrials.gov/show/NCT02594124.
21. A Study to Assess the Safety and Tolerability of Nusinersen (ISIS 396443) in Participants with Spinal Muscular Atrophy (SMA) (EMBRACE). https://ClinicalTrials.gov/show/NCT02462759.
22. A Study of Multiple Doses of Nusinersen (ISIS 396443) Delivered to Infants with Genetically Diagnosed and Presymptomatic Spinal Muscular Atrophy (NUTURE). https://ClinicalTrials.gov/show/NCT02386553.
23. Expanded Access Program (EAP) for Nusinersen in Participants with Infantile-Onset (Consistent with Type 1) Spinal Muscular Atrophy (SMA). https://ClinicalTrials.gov/show/NCT02865109.
24. A Study to Assess the Efficacy and Safety of Nusinersen (ISIS 396443) in Participants with Later-Onset Spinal Muscular Atrophy (SMA) (CHERISH). https://ClinicalTrials.gov/show/NCT02292537.
25. Cerritelli, S.M., and Crouch, R.J. (2009). Ribonuclease H: the enzymes in eukaryotes. FEBS J. *276*, 1494–1505.
26. Bennett, C.F., Baker, B.F., Pham, N., Swayze, E., and Geary, R.S. (2017). Pharmacology of antisense drugs. Annu. Rev. Pharmacol. Toxicol. *57*, 81–105.
27. Hung, G., Xiao, X., Peralta, R., Bhattacharjee, G., Murray, S., Norris, D., Guo, S., and Monia, B.P. (2013). Characterization of target mRNA reduction through in situ RNA hybridization in multiple organ systems following systemic antisense treatment in animals. Nucleic Acid Ther. *23*, 369–378.
28. Kordasiewicz, H.B., Stanek, L.M., Wancewicz, E.V., Mazur, C., McAlonis, M.M., Pytel, K.A., Artates, J.W., Weiss, A., Cheng, S.H., Shihabuddin, L.S., et al. (2012). Sustained therapeutic reversal of Huntington's disease by transient repression of huntingtin synthesis. Neuron *74*, 1031–1044.
29. Rigo, F., Chun, S.J., Norris, D.A., Hung, G., Lee, S., Matson, J., Fey, R.A., Gaus, H., Hua, Y., Grundy, J.S., et al. (2014). Pharmacology of a central nervous system delivered 2′-O-methoxyethyl-modified survival of motor neuron splicing oligonucleotide in mice and nonhuman primates. J. Pharmacol. Exp. Ther. *350*, 46–55.

30. Volpicelli-Daley, L.A., Abdelmotilib, H., Liu, Z., Stoyka, L., Daher, J.P., Milnerwood, A.J., Unni, V.K., Hirst, W.D., Yue, Z., Zhao, H.T., et al. (2016). G2019S-LRRK2 expression augments α-synuclein sequestration into inclusions in neurons. J. Neurosci. *36*, 7415–7427.

31. Tran, H.T., Chung, C.H., Iba, M., Zhang, B., Trojanowski, J.Q., Luk, K.C., and Lee, V.M. (2014). A-synuclein immunotherapy blocks uptake and templated propagation of misfolded α-synuclein and neurodegeneration. Cell Rep. *7*, 2054–2065.

32. Volpicelli-Daley, L.A., Luk, K.C., Patel, T.P., Tanik, S.A., Riddle, D.M., Stieber, A., Meaney, D.F., Trojanowski, J.Q., and Lee, V.M. (2011). Exogenous α-synuclein fibrils induce Lewy body pathology leading to synaptic dysfunction and neuron death. Neuron *72*, 57–71.

33. Herzig, M.C., Kolly, C., Persohn, E., Theil, D., Schweizer, T., Hafner, T., Stemmelen, C., Troxler, T.J., Schmid, P., Danner, S., et al. (2011). LRRK2 protein levels are determined by kinase function and are crucial for kidney and lung homeostasis in mice. Hum. Mol. Genet. *20*, 4209–4223.

34. Hinkle, K.M., Yue, M., Behrouz, B., Dächsel, J.C., Lincoln, S.J., Bowles, E.E., Beevers, J.E., Dugger, B., Winner, B., Prots, I., et al. (2012). LRRK2 knockout mice have an intact dopaminergic system but display alterations in exploratory and motor co-ordination behaviors. Mol. Neurodegener. *7*, 25.

35. Tong, Y., Giaime, E., Yamaguchi, H., Ichimura, T., Liu, Y., Si, H., Cai, H., Bonventre, J.V., and Shen, J. (2012). Loss of leucine-rich repeat kinase 2 causes age-dependent bi-phasic alterations of the autophagy pathway. Mol. Neurodegener. *7*, 2.

36. Luk, K.C., Kehm, V., Carroll, J., Zhang, B., O'Brien, P., Trojanowski, J.Q., and Lee, V.M. (2012). Pathological α-synuclein transmission initiates Parkinson-like neurodegeneration in nontransgenic mice. Science *338*, 949–953.

37. Mao, X., Ou, M.T., Karuppagounder, S.S., Kam, T.I., Yin, X., Xiong, Y., Ge, P., Umanah, G.E., Brahmachari, S., Shin, J.H., et al. (2016). Pathological α-synuclein transmission initiated by binding lymphocyte-activation gene 3. Science *353*, aah3374.

38. Paumier, K.L., Luk, K.C., Manfredsson, F.P., Kanaan, N.M., Lipton, J.W., Collier, T.J., Steece-Collier, K., Kemp, C.J., Celano, S., Schulz, E., et al. (2015). Intrastriatal injection of pre-formed mouse α-synuclein fibrils into rats triggers α-synuclein pathology and bilateral nigrostriatal degeneration. Neurobiol. Dis. *82*, 185–199.

39. Abdelmotilib, H., Maltbie, T., Delic, V., Liu, Z., Hu, X., Fraser, K.B., Moehle, M.S., Stoyka, L., Anabtawi, N., Krendelchtchikova, V., et al. (2017). α-Synuclein fibril-induced inclusion spread in rats and mice correlates with dopaminergic neurodegeneration. Neurobiol. Dis. *105*, 84–98.

40. Hardy, J., Cai, H., Cookson, M.R., Gwinn-Hardy, K., and Singleton, A. (2006). Genetics of Parkinson's disease and parkinsonism. Ann. Neurol. *60*, 389–398.

41. Fraser, K.B., Moehle, M.S., Alcalay, R.N., and West, A.B.; LRRK2 Cohort Consortium (2016). Urinary LRRK2 phosphorylation predicts parkinsonian phenotypes in G2019S LRRK2 carriers. Neurology *86*, 994–999.

42. Fraser, K.B., Rawlins, A.B., Clark, R.G., Alcalay, R.N., Standaert, D.G., Liu, N., and West, A.B.; Parkinson's Disease Biomarker Program Consortium (2016). Ser(P)-1292 LRRK2 in urinary exosomes is elevated in idiopathic Parkinson's disease. Mov. Disord. *31*, 1543–1550.

43. Guerreiro, P.S., Huang, Y., Gysbers, A., Cheng, D., Gai, W.P., Outeiro, T.F., and Halliday, G.M. (2013). LRRK2 interactions with α-synuclein in Parkinson's disease brains and in cell models. J. Mol. Med. (Berl.) *91*, 513–522.

44. Speidel, A., Felk, S., Reinhardt, P., Sterneckert, J., and Gillardon, F. (2016). Leucine-rich repeat kinase 2 influences fate decision of human monocytes differentiated from induced pluripotent stem cells. PLoS ONE *11*, e0165949.

45. Thévenet, J., Pescini Gobert, R., Hooft van Huijsduijnen, R., Wiessner, C., and Sagot, Y.J. (2011). Regulation of LRRK2 expression points to a functional role in human monocyte maturation. PLoS ONE *6*, e21519.

46. Daher, J.P., Pletnikova, O., Biskup, S., Musso, A., Gellhaar, S., Galter, D., Troncoso, J.C., Lee, M.K., Dawson, T.M., Dawson, V.L., and Moore, D.J. (2012). Neurodegenerative phenotypes in an A53T α-synuclein transgenic mouse model are independent of LRRK2. Hum. Mol. Genet. *21*, 2420–2431.

47. Lin, X., Parisiadou, L., Gu, X.L., Wang, L., Shim, H., Sun, L., Xie, C., Long, C.X., Yang, W.J., Ding, J., et al. (2009). Leucine-rich repeat kinase 2 regulates the progression of neuropathology induced by Parkinson's-disease-related mutant alpha-synuclein. Neuron *64*, 807–827.

48. Daher, J.P., Volpicelli-Daley, L.A., Blackburn, J.P., Moehle, M.S., and West, A.B. (2014). Abrogation of α-synuclein-mediated dopaminergic neurodegeneration in LRRK2-deficient rats. Proc. Natl. Acad. Sci. USA *111*, 9289–9294.

49. Skibinski, G., Nakamura, K., Cookson, M.R., and Finkbeiner, S. (2014). Mutant LRRK2 toxicity in neurons depends on LRRK2 levels and synuclein but not kinase activity or inclusion bodies. J. Neurosci. *34*, 418–433.

50. Westerlund, M., Ran, C., Borgkvist, A., Sterky, F.H., Lindqvist, E., Lundströmer, K., Pernold, K., Brené, S., Kallunki, P., Fisone, G., et al. (2008). Lrrk2 and alpha-synuclein are co-regulated in rodent striatum. Mol. Cell. Neurosci. *39*, 586–591.

51. Rudenko, I.N., and Cookson, M.R. (2014). Heterogeneity of leucine-rich repeat kinase 2 mutations: genetics, mechanisms and therapeutic implications. Neurotherapeutics *11*, 738–750.

52. Orenstein, S.J., Kuo, S.H., Tasset, I., Arias, E., Koga, H., Fernandez-Carasa, I., Cortes, E., Honig, L.S., Dauer, W., Consiglio, A., et al. (2013). Interplay of LRRK2 with chaperone-mediated autophagy. Nat. Neurosci. *16*, 394–406.

53. Swayze, E.E., Siwkowski, A.M., Wancewicz, E.V., Migawa, M.T., Wyrzykiewicz, T.K., Hung, G., Monia, B.P., and Bennett, C.F. (2007). Antisense oligonucleotides containing locked nucleic acid improve potency but cause significant hepatotoxicity in animals. Nucleic Acids Res. *35*, 687–700.

54. Rigo, F., Seth, P.P., and Bennett, C.F. (2014). Antisense oligonucleotide-based therapies for diseases caused by pre-mRNA processing defects. Adv. Exp. Med. Biol. *825*, 303–352.

55. Volpicelli-Daley, L.A., Luk, K.C., and Lee, V.M. (2014). Addition of exogenous α-synuclein preformed fibrils to primary neuronal cultures to seed recruitment of endogenous α-synuclein to Lewy body and Lewy neurite-like aggregates. Nat. Protoc. *9*, 2135–2146.

OMTN, Volume *8*

Supplemental Information

LRRK2 Antisense Oligonucleotides Ameliorate α-Synuclein Inclusion Formation in a Parkinson's Disease Mouse Model

Hien Tran Zhao, Neena John, Vedad Delic, Karli Ikeda-Lee, Aneeza Kim, Andreas Weihofen, Eric E. Swayze, Holly B. Kordasiewicz, Andrew B. West, and Laura A. Volpicelli-Daley

Fig. S1

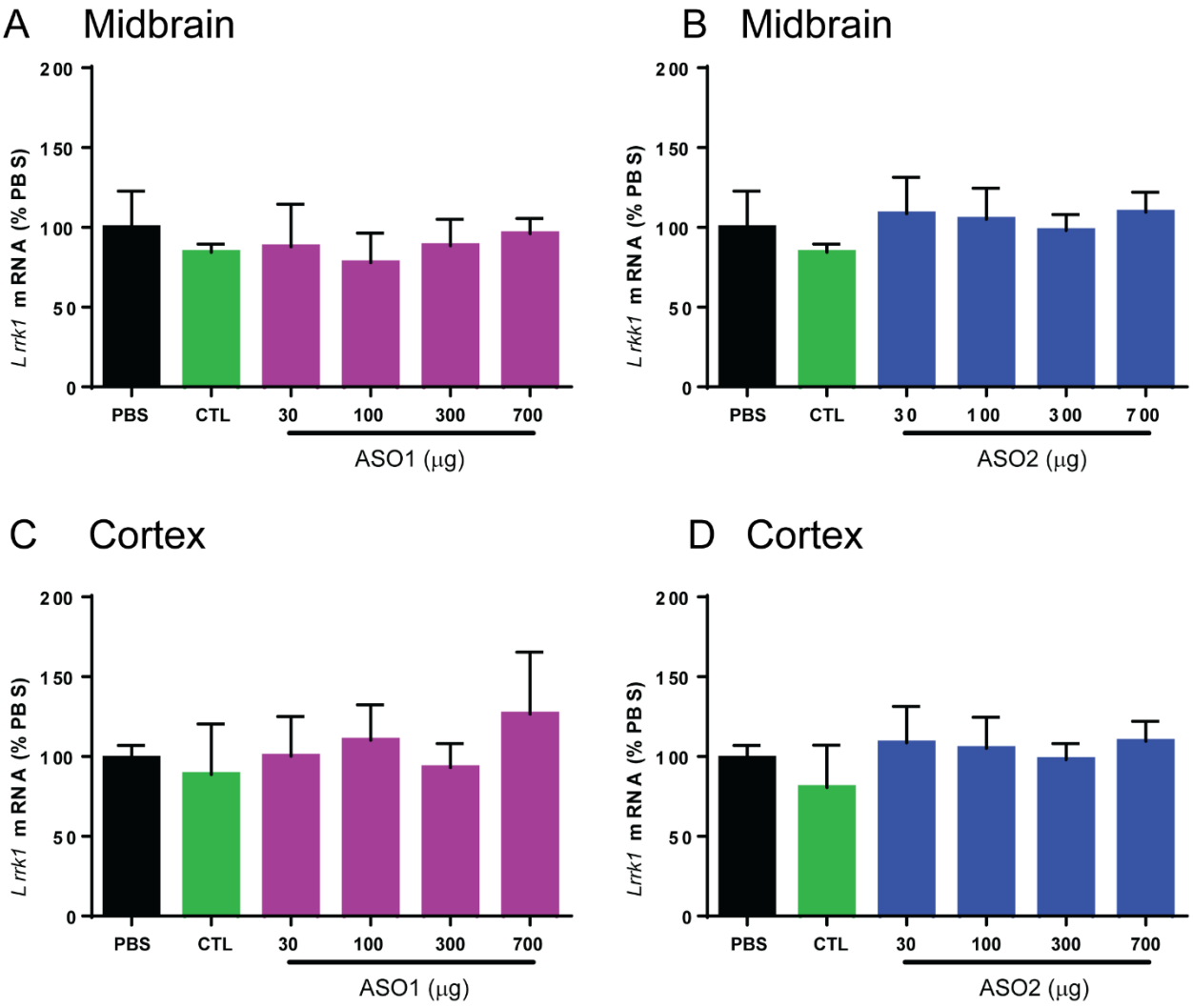

Fig. S1. No change in *Lrrk1* mRNA levels in the midbrain and cortex following LRRK2 ASO treatment. C57BL/6J mice received ICVB treatments with PBS (N=3), 700 µg CTRL (N=3), or LRRK2 ASO1 (N=3), or LRRK2 ASO2 (N=3) at 30, 100, 300 or 700 µg, respectively. Fourteen days later, brains were dissected and *Lrrk1* mRNA was quantified by RT-qPCR in the midbrain (**A,B**) and cortex (**C,D**) Data represents % PBS +/- SEM. LRRK2 ASO-treated groups were compared to PBS or CTL-treated groups using one-way ANOVA with Tukey's post-test.

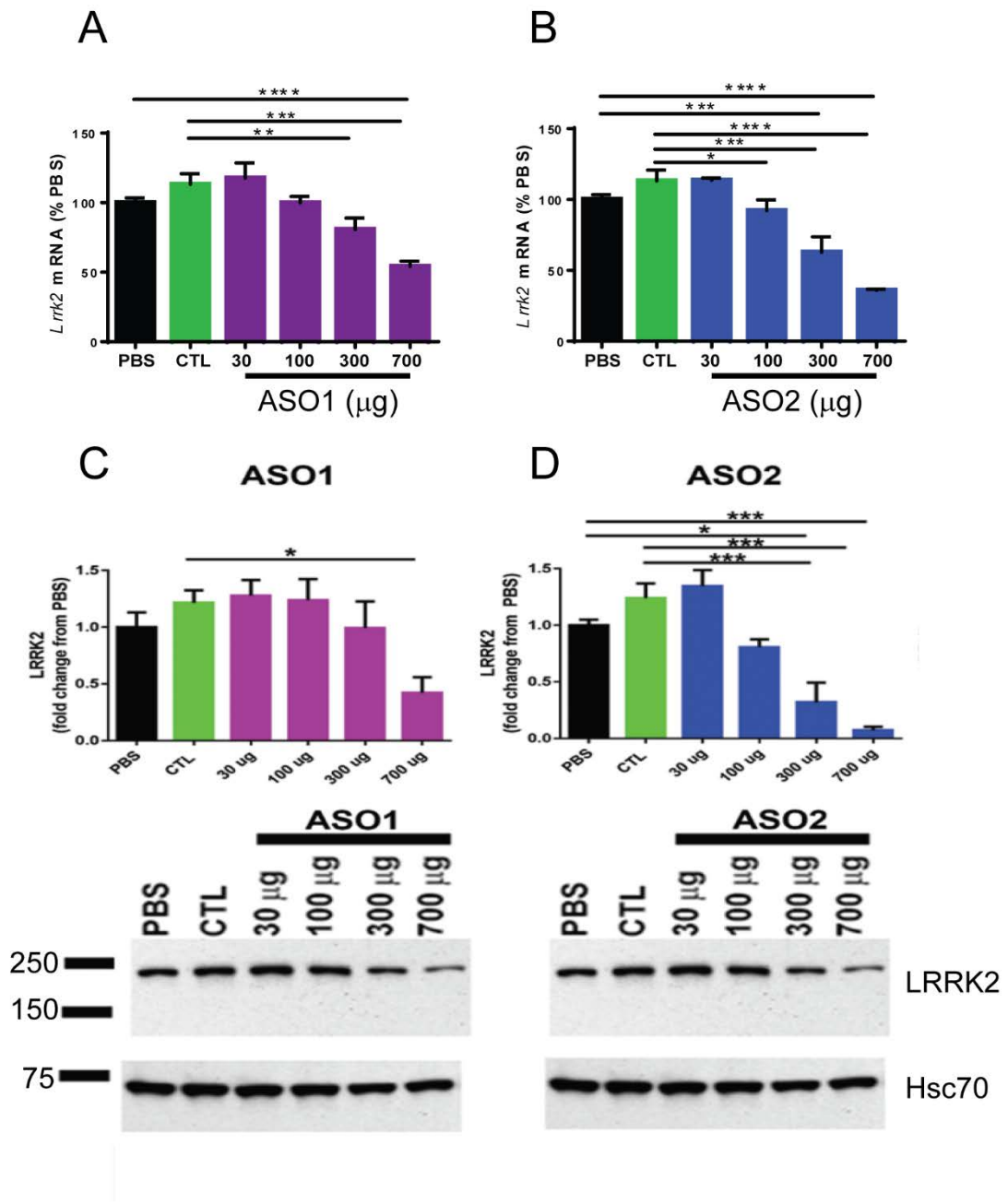

Fig. S2. Dose-dependent reduction of *Lrrk2* mRNA and LRRK2 protein in the cortex in LRRK2 ASO-treated mice. A,B. C57BL/6J mice received ICVB treatments with PBS (N=3), 700 µg CTRL (N=3), or LRRK2 ASO1 (N=3), or LRRK2 ASO2 (N=3) at 30, 100, 300 or 700 µg, respectively. Fourteen days later, brains were dissected. *Lrrk2* mRNA in the cortex was

quantified by RT-qPCR. **C,D.** Cortex homogenates from treated mice were immunoblotted for total LRRK2. HSC70 was used as a loading control. Bands from the LRRK2 immunoblots were quantified using ImageJ and normalized to HSC70. Data represents mean fold change relative PBS +/- SEM. LRRK2 ASO-treated groups were compared to PBS or CTL-ASO groups using one-way ANOVA with Tukey's post-test. * $P < 0.05$, ** $P < 0.01$, and *** $P < 0.001$.

Fig. S3

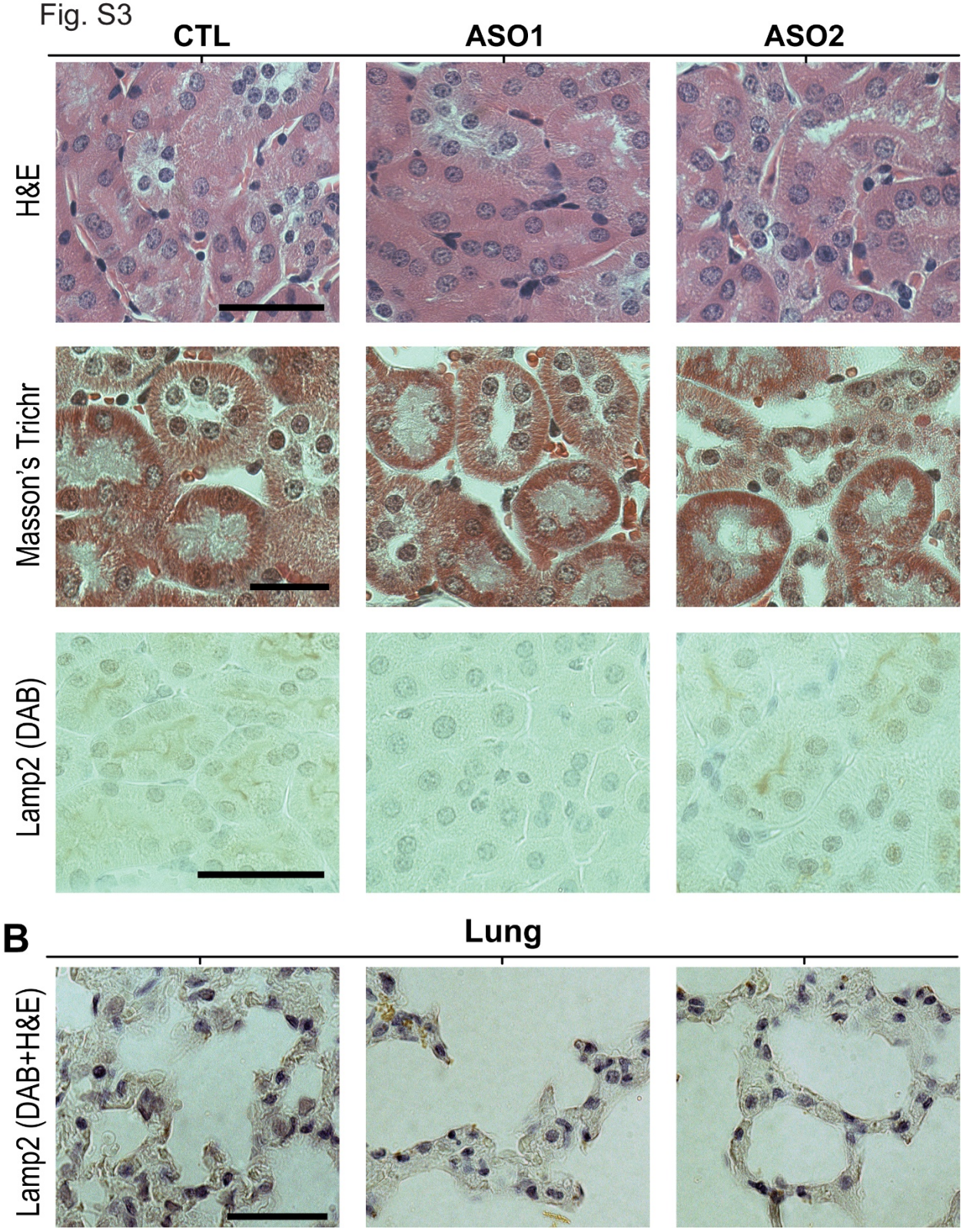

Figure S3. No histological change observed in kidney and lung following central administration of LRRK2-ASOs. **A.** To visualize the presence of vacuoles in proximal kidney epithelial cells, sections from kidney from ICVB treated mice receiving CTRL, LRRK2 ASO1 or LRRK2 ASO2 were stained using H&E, or **B.** Masson's Trichrome stain to visualize protein deposits. **C.** LAMP2 immunohistochemistry was also performed to visualize late endosomes/lysosomes in tubule cells. Sections shown are representative from dozens of sections cut through the kidney and lung from at least three animals from each group. Scale bars are 100 µm.

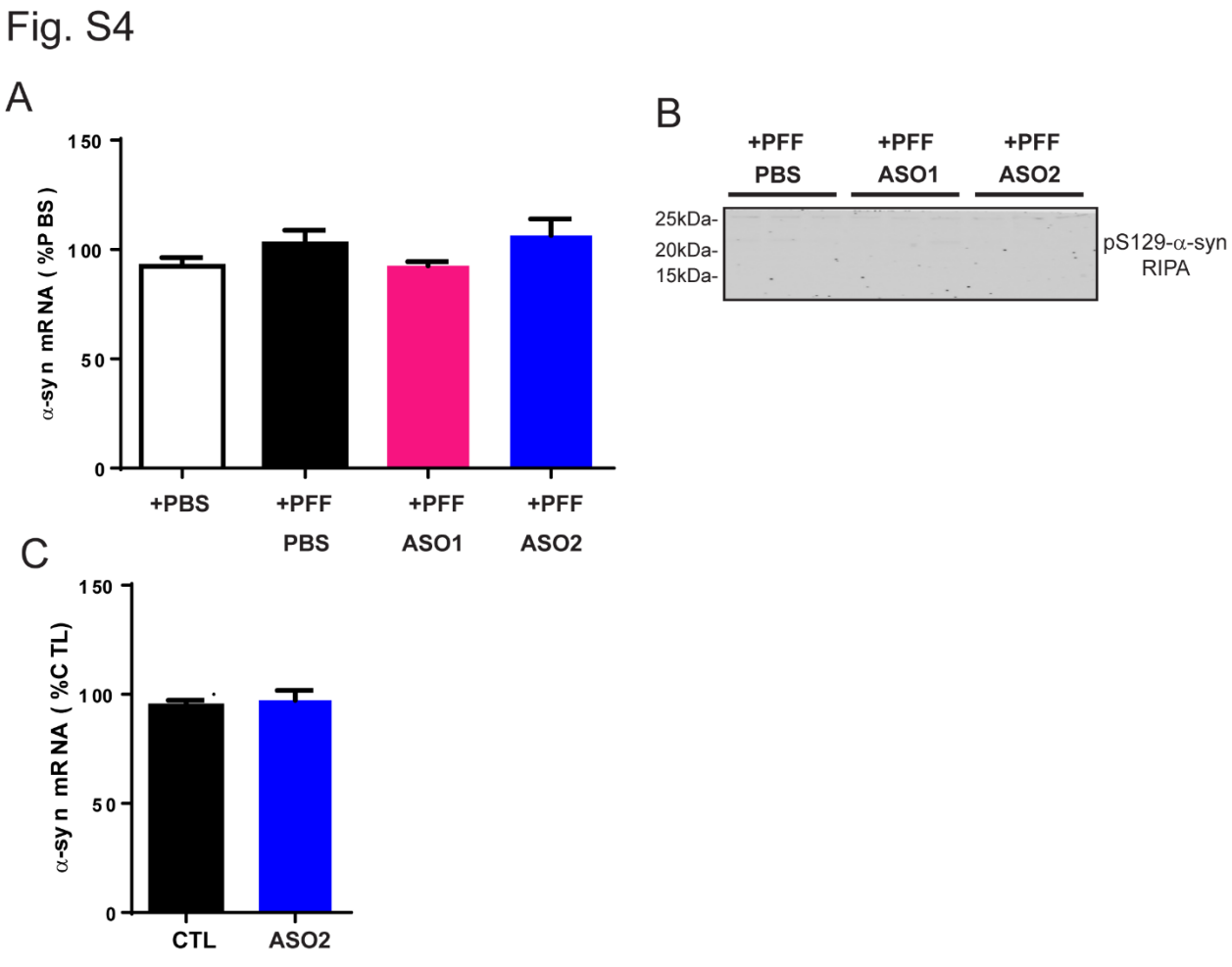

Fig. S4. No change in *SNCA* mRNA levels or RIPA-soluble pS129-α-syn in PFF-injected

mice treated with LRRK2 ASOs. A. Mice received ICVB injections of PBS, LRRK2 ASO1 (700 µg), LRRK2 ASO2 (700 µg). Fourteen days later, 5 µg of PFFs were unilaterally injected into the right striatum. Fifty-six days later, mice were sacrificed. *SNCA* mRNA was assessed in the contralateral midbrain by RT-qPCR (N=11-12). LRRK2 ASO-treated groups were compared to PBS or CTL-treated groups using one-way ANOVA with Tukey's post-test. **B.** Contralateral cortex of PFF injected mice treated with PBS, ASO1 or ASO2 were extracted in RIPA buffer and western blotted with pS129-α-syn for pathological α-syn (N=3 per group). **C.** Mice received ICVB injections of CTL ASO (700 µg) or LRRK2 ASO2 (700 µg). Fourteen days later, 5 µg of PFFs were unilaterally injected into the striatum. Ninety days later, mice received additional ICVB injections of CTL ASO (700 µg) or LRRK2 ASO2 (700 µg). The mice were sacrificed 180 days after the first ASO injection. *SNCA* mRNA was assessed in the midbrain RT-qPCR (N=6). LRRK2 ASO-treated group was compared to CTL group using student's t-test.